Methods

Yeast strains and media

Details of strains used are presented in Table S1. All media were as described [1]. Gene deletions and tag insertions were created by the one-step gene replacement method [2]. The *kanMX6* cassette was, as the need arose, switched to *hygMX6* (*HphMX6*) [3, 4], *his3+* (*his3+ MX6*) or *leu1+* (*kanMX6::leu1+*) [5]. For replacements with *ura4*, fragments were amplified from pKS-ura4 [6]. Multiply mutated genotypes were produced by mating combinations of strains. The synthetic telomere insert strains were constructed as described [7].

For most strains harboring tagged proteins, both mitotic and meiotic cell cycles progress normally. However, strains harboring *pnmt1:GFP-atb2* show an elevated prevalence of meiotic lagging chromosomes in an otherwise wt background (2.5% in wt *versus* 10% in *pnmt1:GFP-atb2*).

Strains harboring *lys1::cnp1-GFP* produce smaller colonies than wt strains in mitotic culture but behave normally in meiosis. When *bqt1* is deleted, the strains with this mild over-expression of Cnp1 show a lower incidence of chromosome-spindle unattachment (23% compared to ~30% in cells expressing wt levels of Cnp1). Hence, perhaps unsurprisingly, mild Cnp1 overexpression partially suppresses the *bqt1Δ* centromere assembly defect.

clr4Δ strains display a mating-type switching deficiency phenotype in homothallic strains [8, 9]. For this reason we included *h+* x *h-* matings of *clr4Δ* and *clr4Δ bqt1Δ* strains in addition to the h^{90} strains. No significant difference was observed between h^{90} or *h+/-* matings.

For experiments examining zygotic meiosis, cells were grown at 32°C in YES media, washed and meiotically induced by incubating h^{90} or a mixture of *h-* and *h+* cells on ME plates at 30°C for approximately 7 hours before starting analysis by live microscopy (described below). For meiotic synchronization of azygotic cells, cultures were grown at 32ºC in YES to a density of $1x10^7$cells/ml, harvested, washed and re-suspended in EMM (+N) and grown at 32°C to a density of $1x10^7$ cells/ml. Cells were harvested, washed three times and re-suspended EMM (-N) +0.5% glucose to a final density of 0.5 x 10^7 cells/ml, and incubated at 30 °C with vigorous shaking for meiotic induction. Zygotes (referred to as meiocytes or meiotic cells throughout the manuscript) were filmed at intervals from 4-7 hours post-meiotic induction.

Table S1

Strains used in this study:

Strain	Genotype	Figure
4583	h90 *leu1-32 ura4-D18 his3-D1 lys1:Pnmt1:GFP-atb2 hht1-mRFP:KanMX6*	1

8461	h90 *leu1-32 ura4-D18 his3-D1 lys1:Pnmt1:GFP-atb2 hht1-mRFP:KanMX6 bqt1::SCleu2+*	1
8916	h90 *leu1-32 ura4-D18 his3-D1 lys1:Pnmt1:GFP-atb2 hht1-mRFP:KanMX6 rap1::ura4+ lig4:: SCleu2+*	1
8490	h90 *Z::NatMX6-Padh31-tetR-Tomato dh1L::tetO*2-ura4 mis6-GFP::KanMX6 lys1::hyg.Br-Pspo55-R-Tspo5 leu1*	1
8906	h90 *Z::NatMX6-Padh31-tetR-Tomato dh1L::tetO*2-ura4 mis6-GFP::KanMX6 lys1::hyg.Br-Pspo55-R-Tspo5 leu1bqt1::SCleu2+*	1
11107	h90 *leu1-32 z:NatR-Padh31-tetR-tomato cnt2:tetO*2:ura4 Sad1-CFP:KanMX6 lys1:cnp1-GFP*	1
11112	h90 *leu1-32 z:NatR-Padh31-tetR-tomato cnt2:tetO*2:ura4 Sad1-CFP:KanMX6 lys1:cnp1-GFP bqt1::SCleu2+*	1
8899	h90 *leu1-32 ura4-D18 his3-D1 hht1-mRFP:KanMX6 Reb1-GFP::NatMX6*	1
8897	h90 *leu1-32 ura4-D18 his3-D1 hht1-mRFP:KanMX6 bqt1::SCleu2+ Reb1-GFP::NatMX6*	1
8932	h90 *leu1-32 ura4-D18 his3-D1 hht1-mrfp:Nat*MX6 lys1:cnp1-GFP-lys1+	2
8935	h90 *leu1-32 ura4-D18 his3-D1 hht1-mrfp:NatMX6*	2

	lys1:cnp1-GFP-lys1+ bqt1::HygMX6	
8945	h90 *Z::NatMX6-Padh31-tetR-Tomato dh1L::tetO*2-ura4+ lys1::HygMX6.Br-Pspo55-R-Tspo5 leu1 swi6-GFP:kanMX6*	2
8992	h90 *Z::NatMX6-Padh31-tetR-Tomato dh1L::tetO*2-ura4+ lys1::HygMX6.Br-Pspo55-R-Tspo5 leu1 swi6-GFP:KanMX6 bqt1:: SCleu2+ ade6-M216*	2
9470	h- *ade6-M210 leu1-32 lys1:Pnmt1:GFP-atb2 hht1-mRFP:KanMX6::leu1+ sid4-GFP:KanMX6 clr4::NatMX6*	3
9472	h+ *ade6-M216 leu1-32 lys1:Pnmt1:GFP-atb2 hht1-mRFP:KanMX6::leu1+ sid4-GFP:KanMX6 clr4::NatMX6*	3
9499	*h+/h- ade6-M210 / ade6-M216 taz1-mCherry:NatMX6/ taz1-mCherry:NatMX6 mis6-GFP:KanMX6/ mis6-GFP:KanMX6*	4
11501	h90 *ade6-M210 leu1-32 ura4::telomere(500bp) his3-D1 taz1-YFP:KanMX6 hht1-CFP:HygMX6 sid4-mCherry:NatMX6 trt1::his3+ aur1::pnda3-mCherry-atb2*	4
8832	h90 *ade6-M210 leu1-32 his7:Pdis1:GFP-LacI-NLS lys1:LacO hht1-mRFP:NatMX6 ura4:telo(500bp) trt1::HygMX6 + pREP1-pnmt1:mRFP-atb2*	4
11667	h90 ade6-M210 leu1-32 his7:Pdis1:GFP-LacI-NLS lys1:LacO hht1-mRFP:NAT ura4:telo(ura500bp) trt1::hygMX6 Bqt1-GBP:KanMX6	4

11172	h90 ade6-M210 leu1-32 his7:Pdis1:GFP-LacI-NLS lys1:LacO hht1-mRFP:NAT bqt1-GBP:kanMX6 pot1::hygMX6	4
10128	h90 ade6-M210 his3-D1 hht1-CFP:his3 pnda3-mCherry-atb2:aur1 sid4-mCherry:natMX6 mis6-GFP:kanMX6 bqt1::hygMX6	S1
8382	h90 *ade6-M216 leu1-32 ura4-D18 lys1-131 dad1::dad1-GFP-HA-KanMX6 hht1-mRFP:NatMX6*	S2
8411	h90 *ade6-M216 leu1-32 ura4-D18 lys1-131 dad1::dad1-GFP-HA-KanMX6 hht1-mRFP:NatMX6 bqt1::HygMX6*	S2
8498	h90 *ade6-M216 leu1-32 ura4-D18 lys1-131 dad1::dad1-GFP-HA-Kanr hht1-mRFP:NatMX6 rap1::ura4+ lig4:: SCleu2+*	S2
8435	h90 *ade6-M210 leu1-32 his7::pdis1::GFP-lacI-NLS lys1:: lacO mis6-mRFP:HygMX6*	S2
8450	h90 *ade6-M210 leu1-32 his7::pdis1::GFP-lacI-NLS lys1:: lacO mis6-mRFP:HygMX6 bqt1:: SCleu2+*	S2
8344	h90 ade6-M216 leu1-32 ura4-D18 lys1-131 nnf1::nnf1-GFP-HA-Kanr Hht1-mRFP-Nat	S3
8357	h90 ade6-M216 leu1-32 ura4-D18 lys1-131 nnf1::nnf1-GFP-HA-Kanr Hht1-mRFP-Nat bqt1::hyg	S3
10263	h90 ade6-M216 leu1-32 ura4-D18 his3-D1 hht1-CFP:his3 pnda3-mCherry-atb2:aur1 sid4-mCherry:natMX6 lys+:cnp1-GFP bqt1::hygMX6	S4
10245	h90 ade6-M216 leu1-32 his3-D1 hht1-CFP:his3 pnda3-mCherry-atb2:aur1 sid4-mCherry:natMX6 swi6-GFP:kanMX6 bqt1::hygMX6	S4

9473	h- *ade6-M210 leu1-32 lys1:Pnmt1:GFP-atb2 hht1-mRFP:KanMX6::leu1+ sid4-GFP:KanMX6* bqt1::HygMX6 clr4::NatMX6	S5
9475	h+ *ade6-M216 leu1-32 lys1:Pnmt1:GFP-atb2 hht1-mRFP:KanMX6::leu1+ sid4-GFP:KanMX6 bqt1::HygMX6 clr4::NatMX6*	S5
10193	h90 *ade6-M210 leu1-32 lys1:Pnmt1:GFP-atb2 hht1-mRFP:KanMX6::leu1+ sid4-GFP:KanMX6 dcr1::NatMX6*	S5
10196	h90 *ade6-M210 leu1-32 lys1:Pnmt1:GFP-atb2 hht1-mRFP:KanMX6::leu1+ sid4-GFP:KanMX6 bqt1::HygMX6 dcr1::NatMX6*	S5
8882	h90 *leu1-32 ura4-D18 his3-D1 hht1-mrfp:NAT lys1:cnp1-GFP-LYS1 dhc1::ura4+*	S6
8884	h90 *leu1-32 ura4-D18 his3-D1 hht1-mrfp:NAT lys1:cnp1-GFP-LYS1 dhc1::ura4+ bqt1:hygMX6*	S6
11601	h90 ade6-M216 leu1-32 ura4-D18 his3-D1 hht1-CFP:his3 pnda3-mCherry-atb2:aur1 sid4-mCherry:natMX6 lys+:cnp1-GFP pot1::hygMX6	S7
8899	h90 *leu1-32 ura4-D18 his3-D1 hht1-mRFP:kanMX6 reb1-GFP::natMX6*	S9
8897	h90 *leu1-32 ura4-D18 his3-D1 hht1-mRFP:kanMX6 reb1-GFP::natMX6 bqt1:: SCleu2+*	S9
11024	h- *trt1::his3 leu1-32 his3-D1 ura4-D18 ade6-M210 hht1-mRFP::NatMX6*	S11
5009	h+ *leu1-32 ura4-D18 his3-D1 lys1:Pnmt1:GFP-atb2 hht1-mRFP:KanMX6*	S11

11506	h90 *ade6-M210 leu1-32 his3-D1 taz1-YFP:KanMX6 hht1-CFP:HygMX6 sod4-mCherry:NatMX6 trt1::his3+ aur1::Pnda3-atb2-mCherry*	S11
10256	h90 *ade6-M210 leu1-32 ura4::telomere(500bp) his3-D1 taz1-YFP:KanMX6 hht1-CFP:HygMX6 sid4-mCherry:NatMX6 trt1::his3+ atb2:Pnmt1:mRFP-atb2-SCleu2+ bqt1::ura4*	S11

Live microscopy

Live analysis was carried out by adhering cells to 35mm glass culture dishes (MatTek) precoated with 0.2 mg/ml soybean lectin (Calbiochem) and immersing them in EMM-N with required supplements (+0.2 mM thiamine for Pnmt1-GFP-Atb2). Cells were imaged on a DeltaVision Spectris (Applied Precision) comprising an Olympus IX71 wide-field inverted fluorescence microscope, an Olympus UPlanSApo 1003, NA 1.35, oil immersion objective, and a Photometrics CCD CH350 camera cooled to -35°C (Roper Scientific), or a DeltaVision Elite (Applied Precision) comprising an Olympus IX71 wide-field inverted fluorescence microscope, an Olympus PLAPON100xO, NA 1.42, oil immersion objective, and a Photometrics CoolSnap HQ2 camera, or a DeltaVision OMX (Applied Precision) comprising an OMX optical microscope (version 4), an Olympus PLAPON60xO, NA 1.42, oil immersion objective, and a sCMOS camera. Culture dishes were incubated at 27°C in the integrated environmental chamber. Images were captured and analyzed using Soft-WoRx (Applied Precision), deconvolved and combined into maximal intensity projections. For long-term timecourse experiments, 9.1 µm of Z-axis imaging was acquired with Optical Axis Integration (OAI). Coverage of the entire cell required a sweep lasting approximately 3 s, and this was repeated every 10 min for approximately 5 hr. For the centromere array experiments we shifted between filter sets on each Z section, before moving on to the next Z section. This way, we avoided the potential problem of centromeres moving during the 3 sec required to sweep the cell. Further experiments showed that due to our scoring system (see below), in which only those centromeres which are well separated in space are scored, there was no significant difference between switching filters between each Z section or between each sweep.

Analysis of kinetochore foci

To assess kinetochore function, we score only those cells displaying proper bipolar spindle formation as evinced by the movement of DNA masses to opposite poles along clearly visible stable spindles in MI and/or MII, or in strains lacking fluorescently tagged tubulin, along the trajectory connecting

SPB signals that move apart symmetrically to opposite poles. The validity of this latter approach was assessed by scoring meiocytes harboring the same kinetochore markers with and without fluorescent tubulin. Kinetochore signals obtained from cells with fluorescent tubulin are fainter due to photobleaching; nevertheless, the effects of bouquet deficiency on kinetochore assembly follow the same pattern in meiocytes with or without tagged tubulin (data not shown). The symmetrical pulling of DNA masses to opposite poles also serves as a marker for spindle formation when no tubulin or SPB markers are present in 'circular' strains (in which all markers are exhausted); note that proper spindle formation is successfully conferred by either the presence of an internal telomere stretch (in the 'circular+internal telo' setting), or a tethered centromere, at the prophase SPB[7] (and AF, AFA, K. Tomita & JPC, submitted).

To assess whether a kinetochore focus co-localizes with a chromatin signal, we quantified imaging data as follows. Images were deconvolved using the DeltaVision Spectris (Applied Precision) software; the resulting images were then analyzed using Volocity software. Background signal values were assigned by averaging the signals associated with two spherical areas inside the cell and subtracted in all further analyses. The background-subtracted intensities of all kinetochore signals co-localizing with DNA masses were then summed. A signal whose intensity was below 1/12 of the total kinetochore signal for a given MI/MII cell was considered undetectable, as the meiotic cell harbors 12 centromeres from late prophase onwards. A chromosome was scored as lacking a kinetochore signal if kinetochore signal associated with that chromosome remained undetectable for at least 3 consecutive frames. Kinetochore signals were scored as stable if they were detectable on chromatin in at least 5 of the first 7 frames after anaphase I or II (frames are taken every 10 min). If the signal could be detected in less than 5 of the first 7 frames after anaphase I or II, it was considered unstable.

Statistical analysis was performed using Fisher's exact test (http://www.langsrud.com/fisher.htm). For kinetochore foci, the fractions of cells lacking stable kinetochore signals were compared among the different genotypes. Therefore, the statistical significance scores express the difference in kinetochore activity between these genotypes.

1 Moreno, S., Klar, A. & Nurse, P. Molecular genetic analysis of fission yeast Schizosaccharomyces pombe. *Methods Enzymol* **194**, 795-823 (1991).

2 Bahler, J. *et al.* Heterologous modules for efficient and versatile PCR-based gene targeting in Schizosaccharomyces pombe. *Yeast* **14**, 943-951, (1998).

3 Hentges, P., Van Driessche, B., Tafforeau, L., Vandenhaute, J. & Carr, A. M. Three novel antibiotic marker cassettes for gene disruption and marker switching in Schizosaccharomyces pombe. *Yeast* **22**, 1013-1019, (2005).

4 Sato, M., Dhut, S. & Toda, T. New drug-resistant cassettes for gene disruption and epitope tagging in Schizosaccharomyces pombe. *Yeast* **22**, 583-591,(2005).

5 Tomita, K. & Cooper, J. P. The telomere bouquet controls the meiotic spindle. *Cell* **130**, 113-126, (2007).

6 Grimm, C., Kohli, J., Murray, J. & Maundrell, K. Genetic engineering of Schizosaccharomyces pombe: a system for gene disruption and replacement using the ura4 gene as a selectable marker. *Mol Gen Genet* **215**, 81-86 (1988).
7 Tomita, K., Bez, C., Fennell, A. & Cooper, J. P. A single internal telomere tract ensures meiotic spindle formation. *EMBO Rep* **14**, 252-260, (2013).
8 Lorentz, A., Ostermann, K., Fleck, O. & Schmidt, H. Switching gene swi6, involved in repression of silent mating-type loci in fission yeast, encodes a homologue of chromatin-associated proteins from Drosophila and mammals. *Gene* **143**, (1994).
9 Bannister, A. J. *et al.* Selective recognition of methylated lysine 9 on histone H3 by the HP1 chromo domain. *Nature* **410**, 120-124, (2001).

Figure S1: **Bouquet deficient meiocytes show failure of chromosome attachment to correctly formed spindles.**

(A-C) Examples of bouquet-deficient cells undergoing meiosis. Tubulin and histone H3 are observed *via* ectopically expressed GFP-Atb2 (green) and endogenous mRFP tagging of one of the two alleles encoding Hht1 (red), respectively. Numbers below frames represent minutes before or after metaphase I. Scale bars represent 5μm.
(D-E) Tubulin and histone H3 are observed *via* endogenously tagged Atb2-mRFP (red) and endogenous CFP tagging of one of the two alleles encoding Hht1 (blue), respectively. Labels as in (A).

(A-B, D-E) *bqt1Δ* meiosis. The spindle forms correctly but some chromosomes (arrows) fail to attach to those spindles and remain unsegregated

(C) *rap1Δ* meiosis. The spindle forms correctly but some chromosomes (arrows) fail to attach to those spindles and remain unsegregated.

(F) Bouquet deficient cells form spindles with normal elongation rates.
The time from anaphase I onset to the moment of maximal spindle length was measured. Red dots represent values for each individual cell; black lines represent the mean +/- standard error. Wt and *bqt1Δ* cells with good spindles have identical maximal spindle lengths and rates of spindle elongation.

Figure S2: **Bouquet deficient meiocytes show incomplete recruitment of Dad1 and Mis6 to centromeres.**

(A,B) Failed Dad1 and Mis6 localization in the absence of the bouquet.

(A) wt meiosis. Dad1-GFP appears at all chromatin masses at MI and MII.
(B) *bqt1Δ* meiosis. Some chromosomes (arrows) fail to recruit Dad1 and remain unsegregated.
(C) Endogenously tagged functional Mis6-GFP is observed along with *cenI-TetO/R*. wt meiosis. Mis6-GFP is correctly recruited to centromere I.
(D) *bqt1Δ* meiosis. In some cases centromere I fails to recruit Mis6 and remains unsegregated.
(E) Quantitation of Dad1 localization. For each genetic background, the percentage of cells harbouring unsegregated chromosomes is plotted; the superimposed colour code specifies the pattern of Dad1-GFP signal in those cells. See Methods for definitions of 'stable' and 'unstable'. Asterisks indicate significant difference from wt calculated using Fisher's exact test (wt-*bqt1Δ* $p=10^{-8}$, wt-*rap1Δ* $p=2*10^{-5}$; see Methods).
(F) Quantitation of Mis6 localization on centromere I. The percentage of cells harbouring unsegregated centromere I is plotted; the superimposed colour code specifies the pattern of Mis6-GFP signal on those centromeres. Number of cells filmed is indicated above each lane. Asterisk indicates significant difference from wt calculated using Fisher's exact test (wt- *bqt1Δ* p=0.04).

Figure S3: **Bouquet deficient meiocytes fail to properly assemble kinetochores.**

(A-C) Nnf1 and chromosomes are observed *via* endogenously tagged functional Nnf1-GFP and Hht1-mRFP (as in Fig. 1), respectively. Nnf1 disappears from centromeres in early prophase and relocalizes to centromeres 10-40 minutes before metaphase I. Labels as in Fig S1.

(A) wt meiosis. Nnf1-GFP appears on all chromatin masses at MI and MII.

(B-C) *bqt1Δ* meiosis. Some chromosomes fail to recruit Nnf1 and remain unsegregated (arrows).

(D) Quantitation of Nnf1 localization. For each genetic background, the percentage of cells harbouring unsegregated chromosomes is plotted; the superimposed colour code specifies the pattern of Nnf1-GFP signal in those cells. See Methods for definitions of 'stable' and 'unstable'. Labels as in Fig S1 (wt-*bqt1Δ* p=0.0014).

Figure S4: **Centromere assembly failure occurs not only in meiocytes with functional spindles, but also in those with dysfunctional spindles.**

In these three examples, SPBs are scattered far from chromatin and spindles fail to assemble properly. Some chromosomes lacking kinetochore signals (either Cnp1 or Swi6; arrows) can be discerned as they separate from the main chromatin mass.

Figure S5: **meiocytes deficient in pericentromeric heterochromatin formation, show centromere assembly defects.**

(A) Genetic epistasis analysis of mutations that abolish the bouquet or compromise heterochromatin assembly. Cumulative frequencies of non-attachment events in MI and MII are observed *via* GFP-Atb2, Sid4-GFP and Hht1-mRFP (as in Fig 1). Asterisks indicate that all mutant backgrounds differ significantly from wt; no significant difference is observed among the various mutant genotypes. Significance was calculated using Fisher's exact test (wt-*bqt1Δ* $p=5*10^{-5}$, wt-*clr4Δ* p=0.002, wt-*clr4 Δ bqt1 Δ* p=0.0005, wt- *dcr1 Δ* p=0.01, wt-*dcr1 Δ bqt1 Δ* p=0.0001, see Methods for details).

(B) Series of frames of a film of a cell undergoing meiosis. Cnp1, tubulin and chromatin are observed *via* ectopically expressed Cnp1-GFP (green) atb2-mCherry (red) and Hht1-CFP (blue), respectively. Numbers below frames represent minutes before or after metaphase I. Scale bars represent 5μm. This film shows an example of *clr4Δ* meiosis. Some chromosomes (arrows) fail to recruit cohesin and thus missegregate, while maintaining high levels of Cnp1.

Figure S6: **Impaired kinetochore assembly is not a result of horsetail movement or reduced meiotic recombination.**

Cnp1-chromatin association was assessed as in Fig 2 in cells lacking Dhc1,which is required for robust meiotic prophase nuclear ('horsetail') movements. In *dhc1Δ* meiocytes, bouquet formation occurs but levels of meiotic recombination are reduced.

(A-B) Cnp1 and chromatin were assessed as in Fig. 2.. These examples show *dhc1Δ bqt1Δ* cells with chromatin masses failing to attach to the spindle and lacking a stable Cnp1-GFP signal (arrows).

(C) Quantitation of Cnp1 localization. For each genetic background, the percentage of cells harbouring unsegregated chromosomes is plotted; the superimposed colour code specifies the pattern of Cnp1-GFP signal in those cells. See Methods for definitions of 'stable' and 'unstable'. (wt-*bqt1Δ* p=0.0003, wt-*bqt1Δ dhc1Δ* p=0.0001, wt-*dhc1Δ* n.s, see Methods for details). In *dhc1Δ* meiocytes, all unsegregated chromosomes show a stable Cnp1-GFP focus. In *dhc1Δ bqt1Δ* meiocytes, a subset of centromeres remain associated with the SPB throughout meiotic prophase. However, the occurrence of unsegregated chromatin masses lacking Cnp1-GFP is not suppressed.

Figure S7: **Impaired kinetochore function in circular chromosome strains.**

Kinetochores are observed via ectopically expressed Cnp1-GFP.
Circular chromosome-containing meiocytes suffer similar phenotypes to bouquet-deficient linear chromosome-containing meiocytes. In these examples, spindles form properly but some chromosomes (arrows) lack kinetochore signals and fail to attach. The top two series show MI missegregation, and the bottom shows an unsegregated chromatid at MII.

Figure S8: **Telomere-centromere proximity confers the ability of the bouquet to promote centromere assembly.**

(A) Diagram of 'circular' genome assessed in (B). The pink ellipse on Chr III represents an internal telomere repeat tract, which is visualized *via* bound Taz1-YFP.

(B) Cells harbor endogenously tagged and functional alleles of Taz1 and Sid4 (a SPB protein), as well as tagged tubulin and histone H3 as in Fig S1. Unsegregated chromosomes (white arrows) do not show Taz1 signal. Fig 4B summarizes the data derived from these and other examples.

(C) Diagram of circular genome assessed in (D). The pink ellipse on Chr III represents an internal telomere repeat tract. The green ellipse represents *cenI-LacO/I*.

(D) Series of frames from a representative film of 'circular+internal telo' cells undergoing meiosis. Chr I is observed via *cenI-LacO/I* (as in Fig 4); tubulin (*atb2*+) and histone H3 observed as in Fig 1. The two Chr I homologs (white arrow) have failed to

attach to the spindle. Fig 4C summarizes the data derived from these and other examples.

Figure S9: **Chr III is not inherently protected from centromere assembly defects.**

A potential alternative explanation for the attachment of ChrIII to the spindle in a 'circular + internal telo' background could stem from the unique presence on Chr III of the rDNA repeats, whose heterochromatic nature could conceivably protect the centromere of Chr III from effects of bouquet deficiency. To assess this possibility, we monitored the attachment of Chr III to the spindle in linear chromosome-containing *bqt1Δ* meiocytes *via* endogenously GFP-tagged and functional Reb1, a rDNA binding protein. Of 29 cells with functional spindles, 10 had chromosomes remaining in the center of the cell at anaphase I or II. In 4 of these 10, the unsegregated chromosome harboured Reb1 signal, indicating that the centromere of Chr III does not enjoy singular protection from non-attachment; rather, the internal telomere stretch affords proper kinetochore assembly on circular Chr III.
Representative films are shown. Numbers below frames represent time relative to metaphase I. Scale bar represents 5μm. Chr III resides in the middle of the cell at anaphase I (arrow), indicating failed segregation.

Figure S10: **Rescue of failed centromere function of Chr I by its tethering to the SPB.**

(A,B) Series of frames from representative films of 'circular+internal telo' cells undergoing meiosis. Chr I is observed via *CenI- LacO/I* (as in Fig 4) and histone H3 is observed as in Fig 1. Note the recruitment of ChrI (green dot) to the SPB (end of the chromatin streak), and the subsequent attachment of the chromosomes to the spindle. MII in 'circular' strains is difficult to visualize clearly since entangled chromatin masses quickly collapse onto each other immediately upon spindle dissolution. Fig 4D summarizes the data derived from these and other examples; hence, only unambiguous segregation (or missegregation) events, during MI, were scored.

Figure S11: **Linear correlation between number of telomeres participating in the bouquet and non-attachment phenotype.**

(A) Mating of a strain harbouring circular chromosomes with a wt strain yields a meiocyte in which three (linear) chromosomes associate with the bouquet and three (circular) chromosomes do not. This meiocyte corresponds to point II in (B).

(B) Positive linear correlation between the number of chromosomes devoid of telomeres attaching to the SPB in a given cell and the percentage of cells with a non-functional centromere. Five strains were scored:

I- cells derived from mating wt strains (all chromosomes participate in the bouquet, therefore no chromosomes are detached from the SPB, n=87).
II- cells depicted in (A), harbouring three linear (telomere-containing) and three circular (telomere-less) chromosomes (n=82).

III- cells from mating of two 'circular+internal telo' strains (see text) of opposite mating type (only two chromosomes participate in the bouquet and therefore 4 chromosome are detached from the SPB in this genetic makeup, n=94).
IV-same as III, but with deletion of *bqt1+,* which leads to abrogation of binding of the internal telomere to the SPB (no telomeres participate in the bouquet and therefore 6 chromosomes are detached from the SPB, n=55).
V- cells from mating of two circular chromosome-containing strains entirely lacking telomere sequences (no telomeres participate in the bouquet and therefore 6 chromosomes are detached from the SPB , n=25).
The dotted line is a linear fit, R^2=0.87.

Figure S12: **Impaired kinetochore function in cases of localization of centromeres to the SPB without the presence of telomeres.**

Endogenously tagged Sad1-CFP (which localizes to the SPB) (blue) is observed along with Centromere II (red, visualized *via* the *cenII -tetO/R*) or Centromere I (green, visualized *via* the *cenI-lacO/I*). Note co-localization of centromere and SPB throughout prophase, and the subsequent non-attachment phenotype of *cenII* or *cenI* (arrows).

FIGURE S1

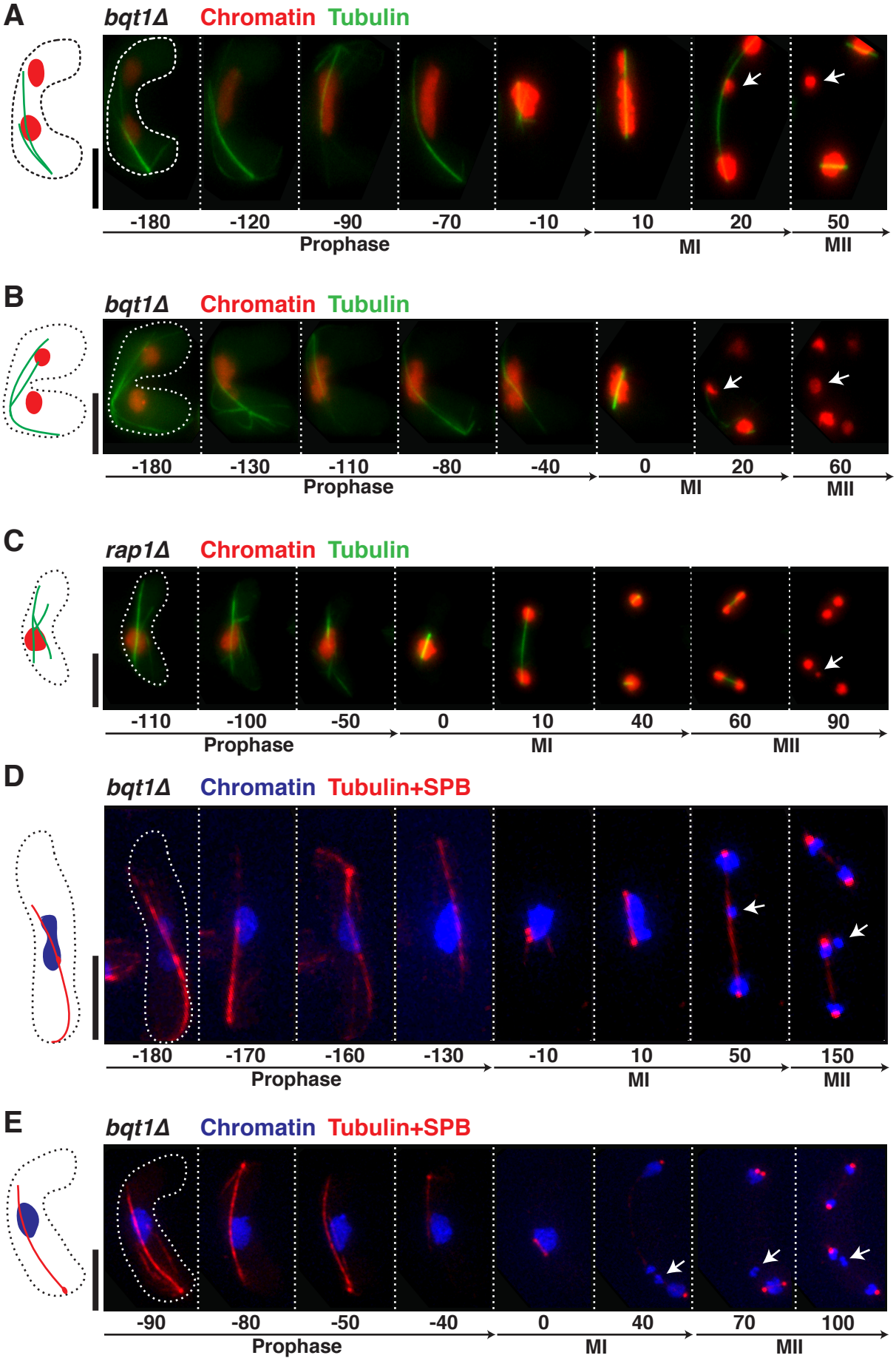
A
bqt1Δ Chromatin Tubulin
-180 -120 -90 -70 -10 10 20 50
Prophase MI MII
B
bqt1Δ Chromatin Tubulin
-180 -130 -110 -80 -40 0 20 60
Prophase MI MII
C
rap1Δ Chromatin Tubulin
-110 -100 -50 0 10 40 60 90
Prophase MI MII
D
bqt1Δ Chromatin Tubulin+SPB
-180 -170 -160 -130 -10 10 50 150
Prophase MI MII
E
bqt1Δ Chromatin Tubulin+SPB
-90 -80 -50 -40 0 40 70 100
Prophase MI MII

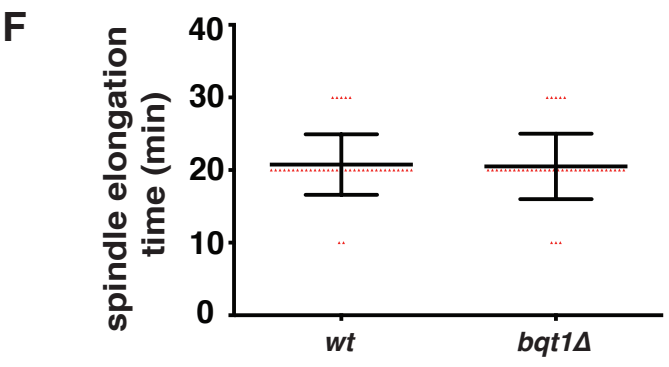
F
spindle elongation time (min)
40
30
20
10
0
wt
bqt1Δ

FIGURE S2

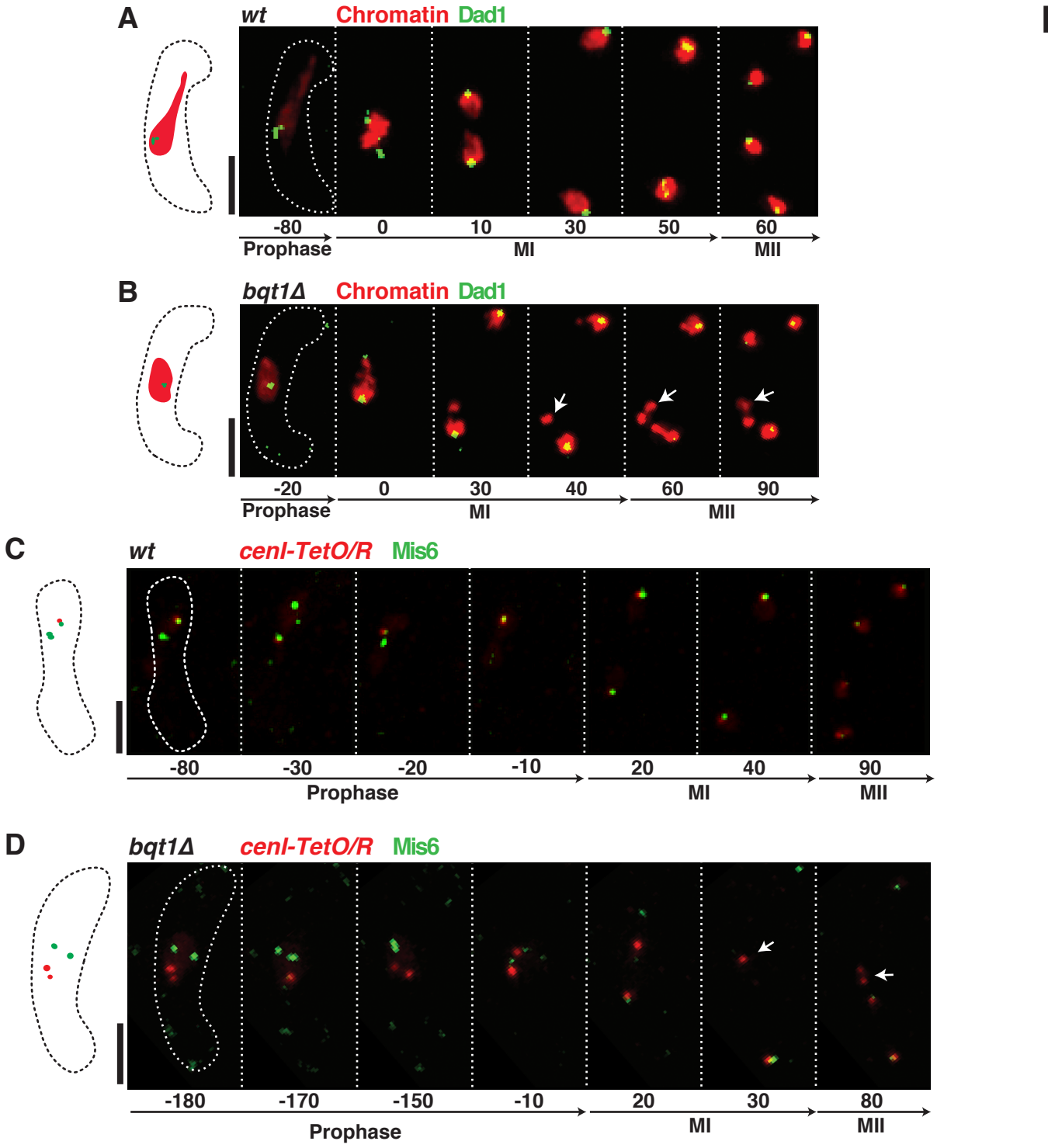
A
wt
Chromatin
Dad1
-80
0
10
30
50
60
Prophase
MI
MII
B
bqt1Δ
Chromatin
Dad1
-20
0
30
40
60
90
Prophase
MI
MII
C
wt
cenI-TetO/R
Mis6
-80
-30
-20
-10
20
40
90
Prophase
MI
MII
D
bqt1Δ
cenI-TetO/R
Mis6
-180
-170
-150
-10
20
30
80
Prophase
MI
MII

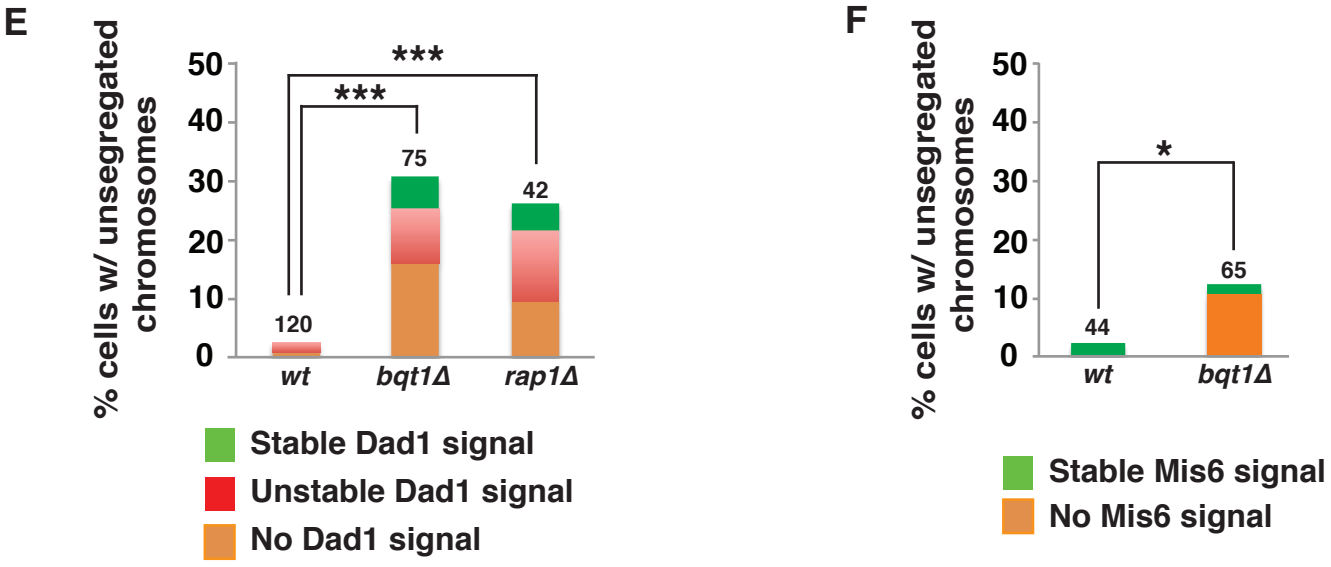
E
% cells w/ unsegregated chromosomes
50
40
30
20
10
0
***
***
75
42
120
wt
bqt1Δ
rap1Δ
Stable Dad1 signal
Unstable Dad1 signal
No Dad1 signal
F
% cells w/ unsegregated chromosomes
50
40
30
20
10
0
*
65
44
wt
bqt1Δ
Stable Mis6 signal
No Mis6 signal

FIGURE S3

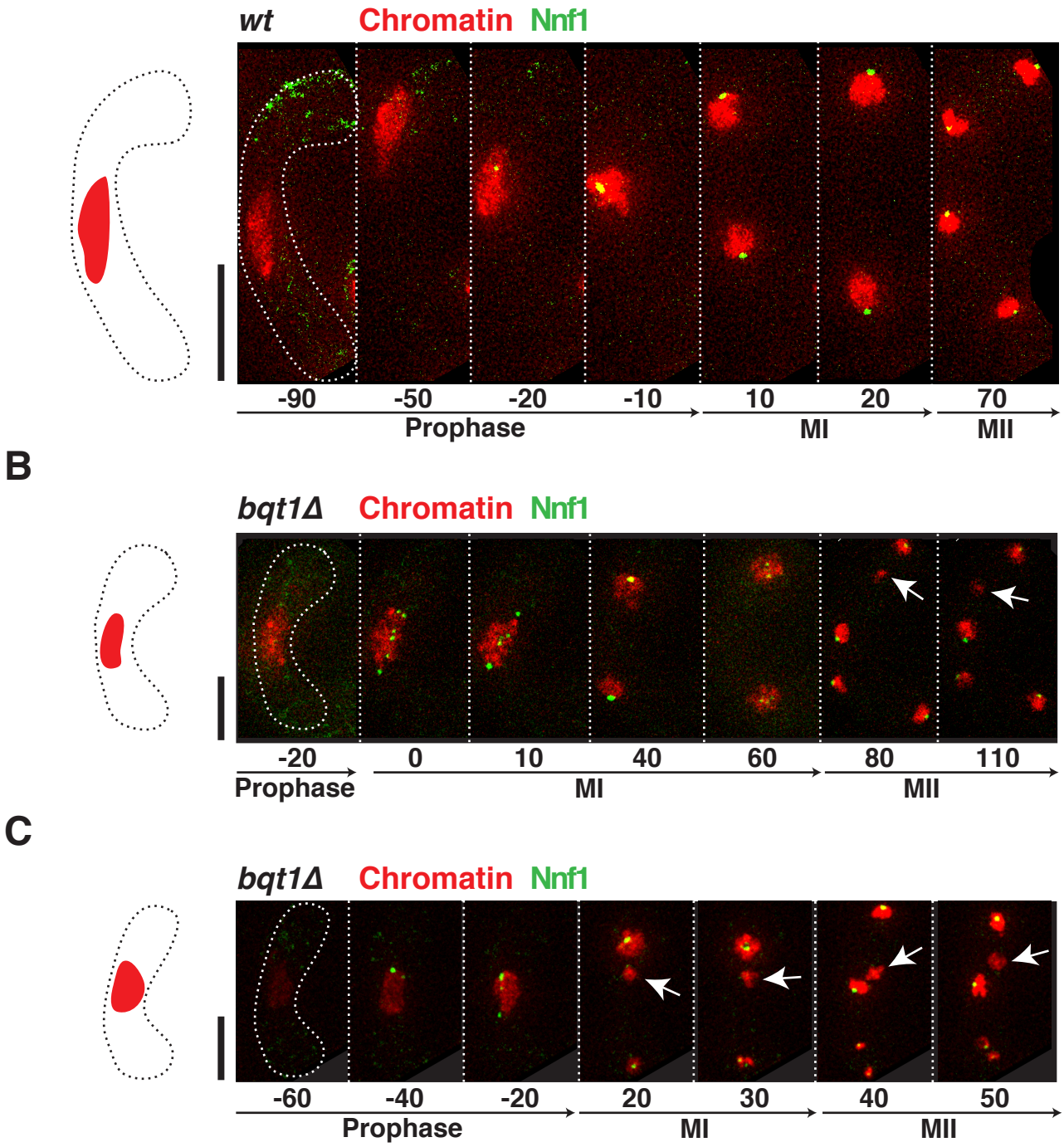
A
wt
Chromatin
Nnf1
-90
-50
-20
-10
10
20
70
Prophase
MI
MII
B
bqt1Δ
Chromatin
Nnf1
-20
0
10
40
60
80
110
Prophase
MI
MII
C
bqt1Δ
Chromatin
Nnf1
-60
-40
-20
20
30
40
50
Prophase
MI
MII

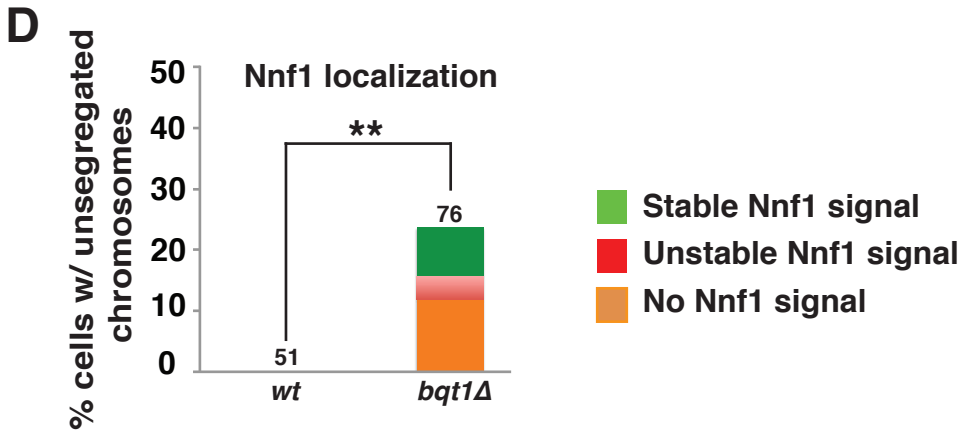
D
% cells w/ unsegregated chromosomes
Nnf1 localization
50
40
30
20
10
0
**
76
51
wt
bqt1Δ
Stable Nnf1 signal
Unstable Nnf1 signal
No Nnf1 signal

FIGURE S4

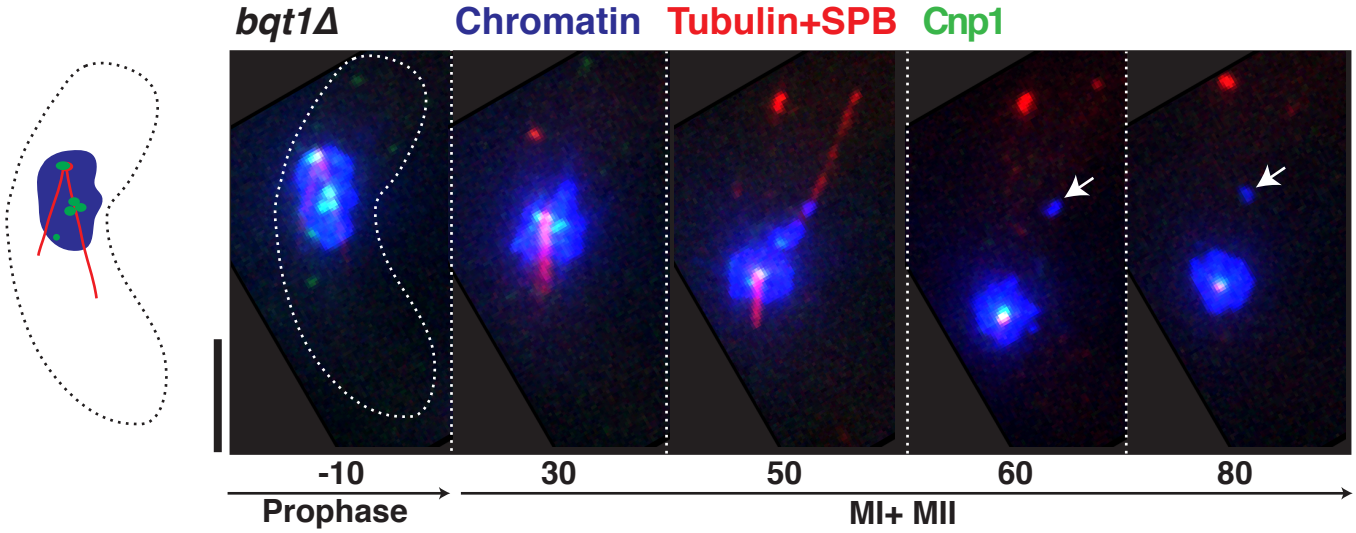
bqt1Δ
Chromatin
Tubulin+SPB
Cnp1
-10
30
50
60
80
Prophase
MI+ MII

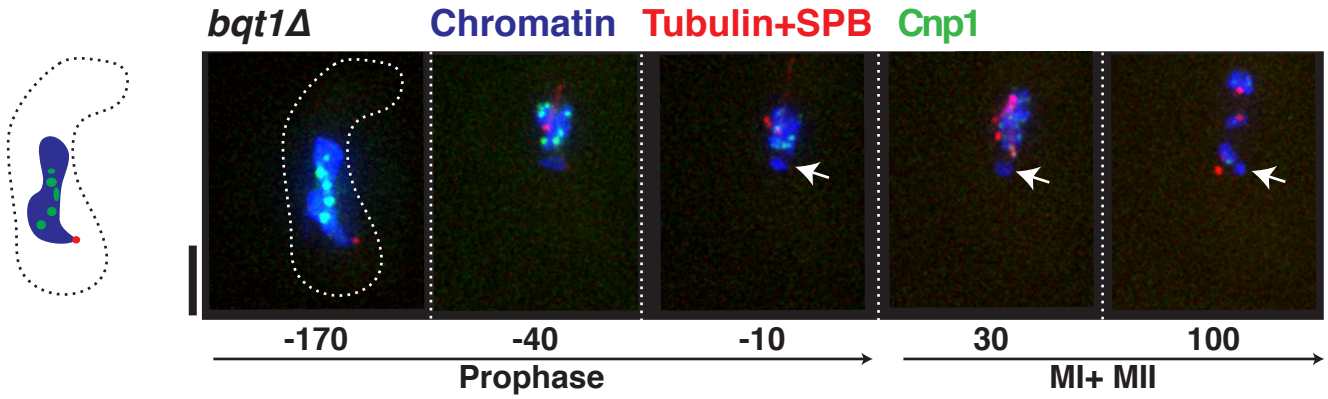
bqt1Δ
Chromatin
Tubulin+SPB
Cnp1
-170
-40
-10
30
100
Prophase
MI+ MII

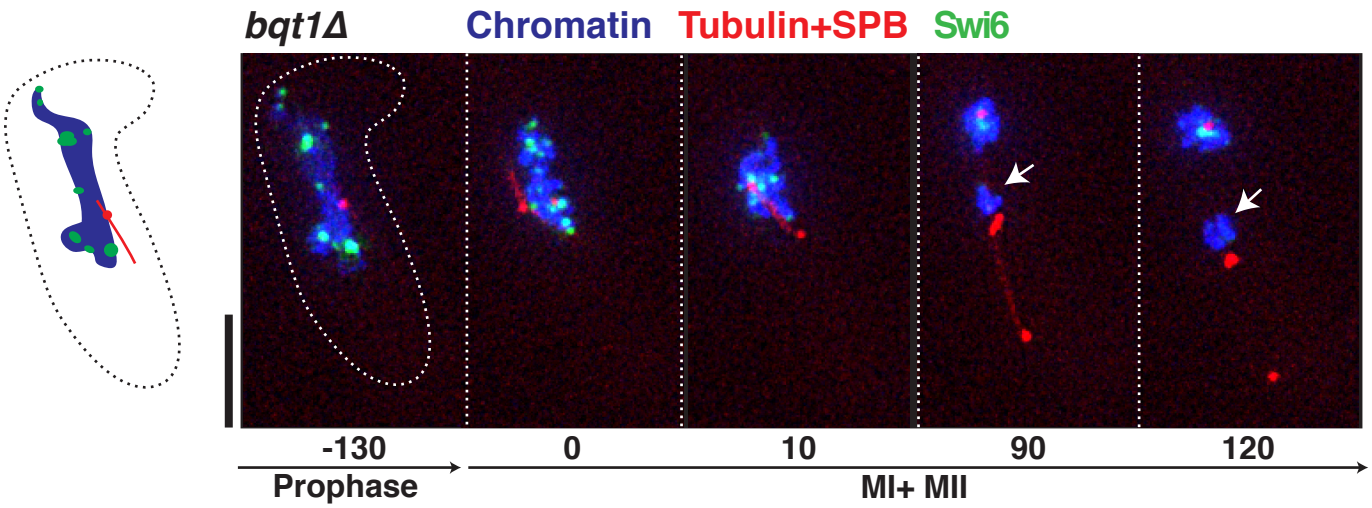
bqt1Δ
Chromatin
Tubulin+SPB
Swi6
-130
0
10
90
120
Prophase
MI+ MII

FIGURE S5

A

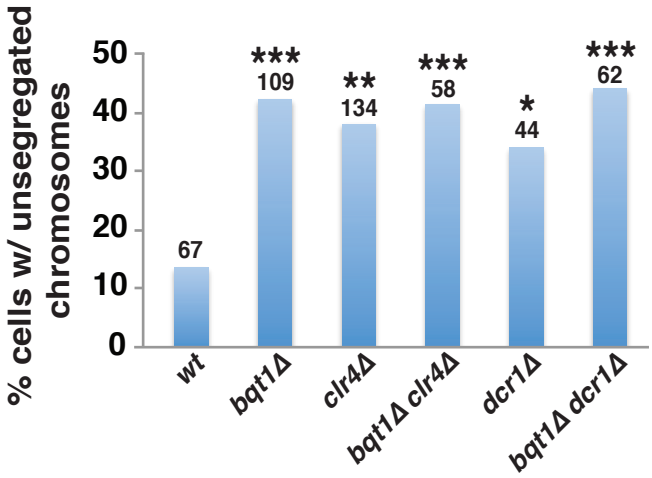
% cells w/ unsegregated chromosomes
50
40
30
20
10
0
67
***
109
**
134
***
58
*
44
***
62
wt
bqt1Δ
clr4Δ
bqt1Δ clr4Δ
dcr1Δ
bqt1Δ dcr1Δ

B

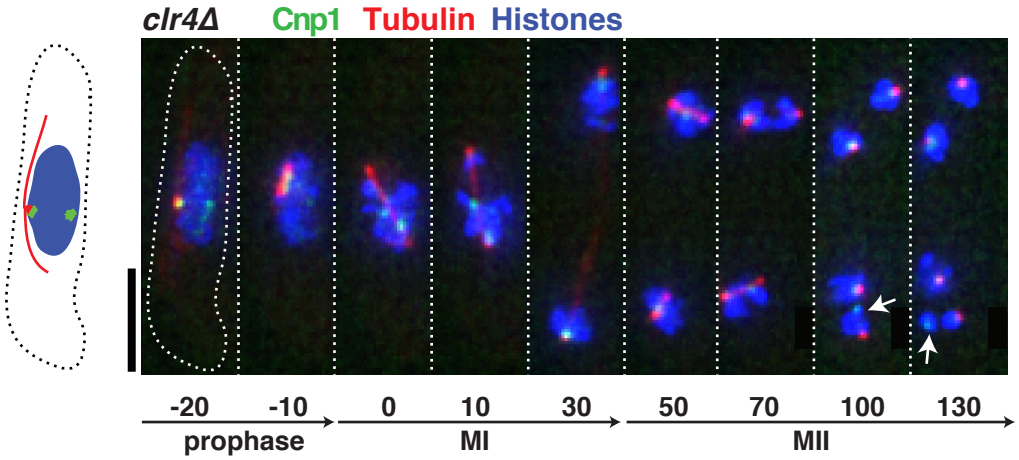
clr4Δ
Cnp1
Tubulin
Histones
-20
-10
0
10
30
50
70
100
130
prophase
MI
MII

A

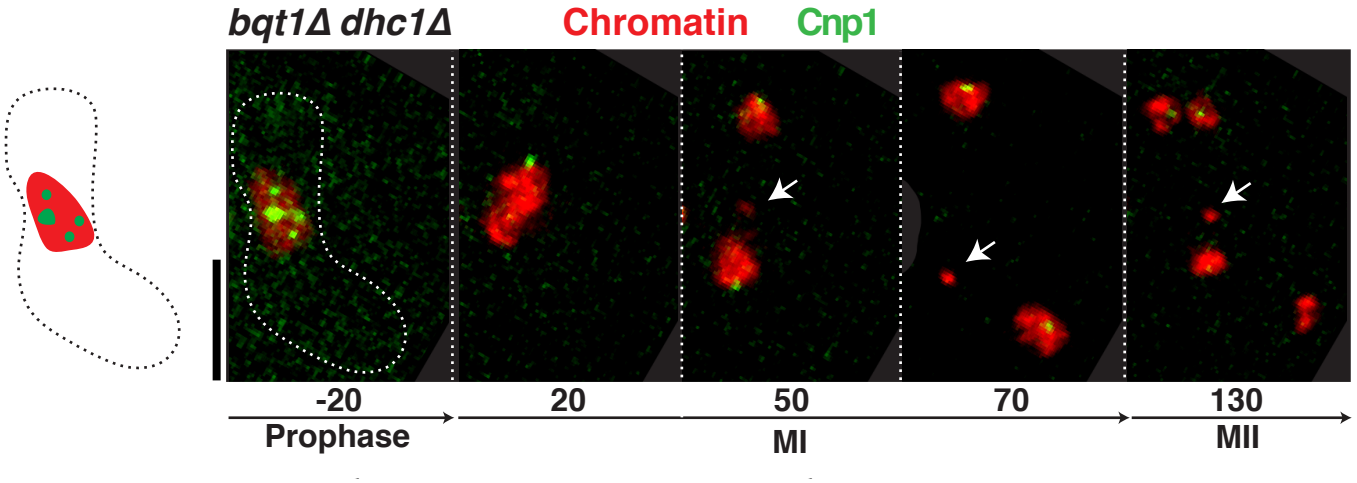
bqt1Δ dhc1Δ
Chromatin
Cnp1
-20
Prophase
20
50
70
MI
130
MII

B

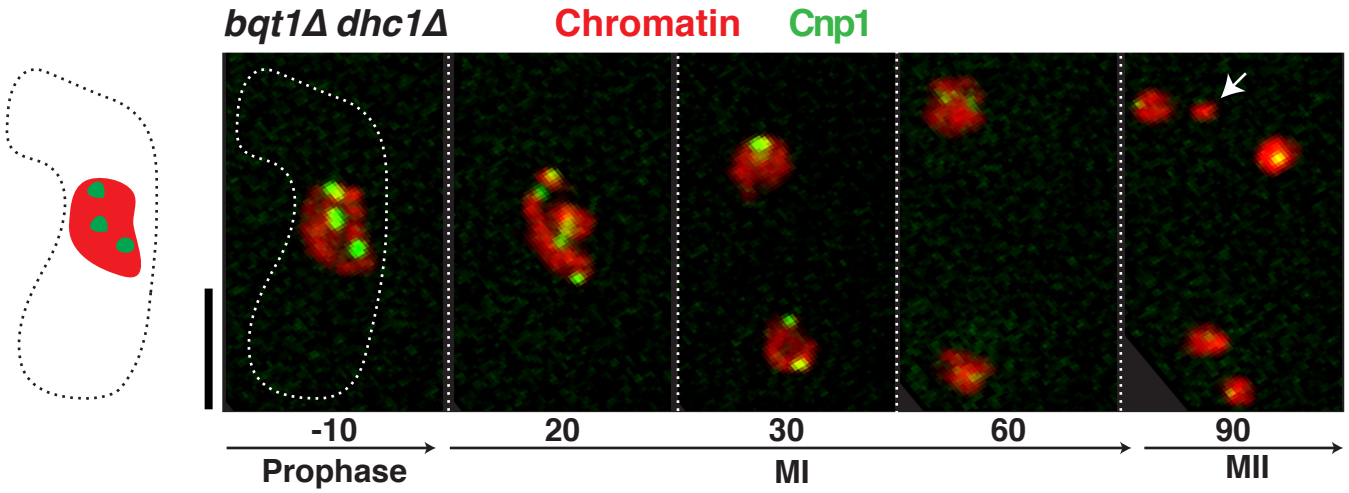
bqt1Δ dhc1Δ
Chromatin
Cnp1
-10
Prophase
20
30
60
MI
90
MII

C

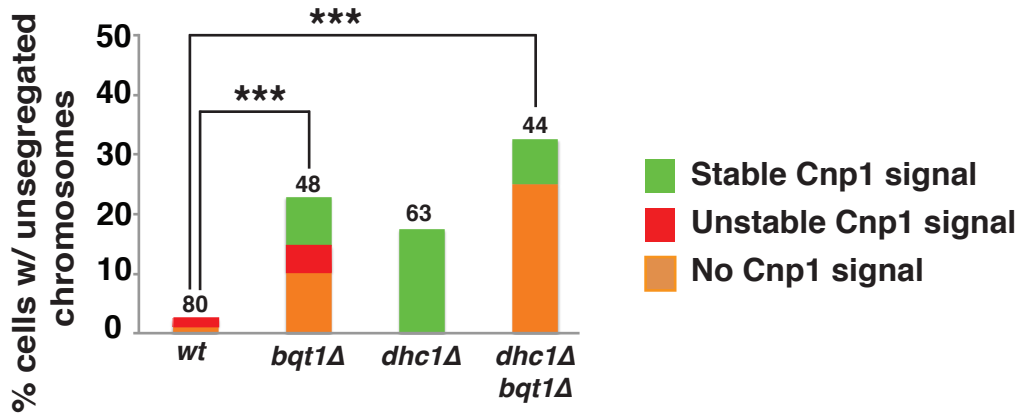
% cells w/ unsegregated chromosomes
50
40
30
20
10
0
***
***
80
48
63
44
wt
bqt1Δ
dhc1Δ
dhc1Δ bqt1Δ
Stable Cnp1 signal
Unstable Cnp1 signal
No Cnp1 signal

FIGURE S7

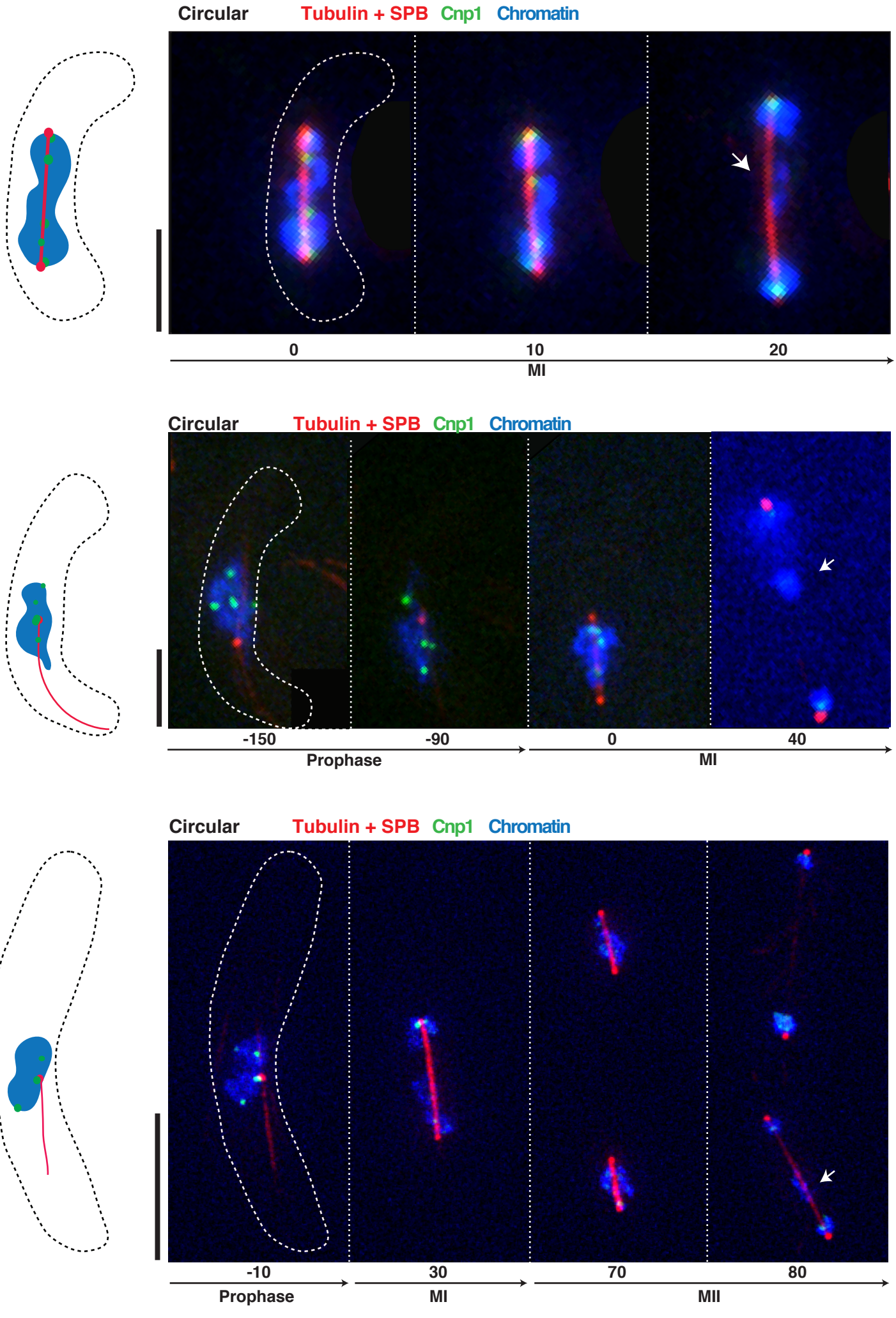
Circular
Tubulin + SPB
Cnp1
Chromatin
0
10
20
MI
Circular
Tubulin + SPB
Cnp1
Chromatin
-150
-90
0
40
Prophase
MI
Circular
Tubulin + SPB
Cnp1
Chromatin
-10
30
70
80
Prophase
MI
MII

FIGURE S8

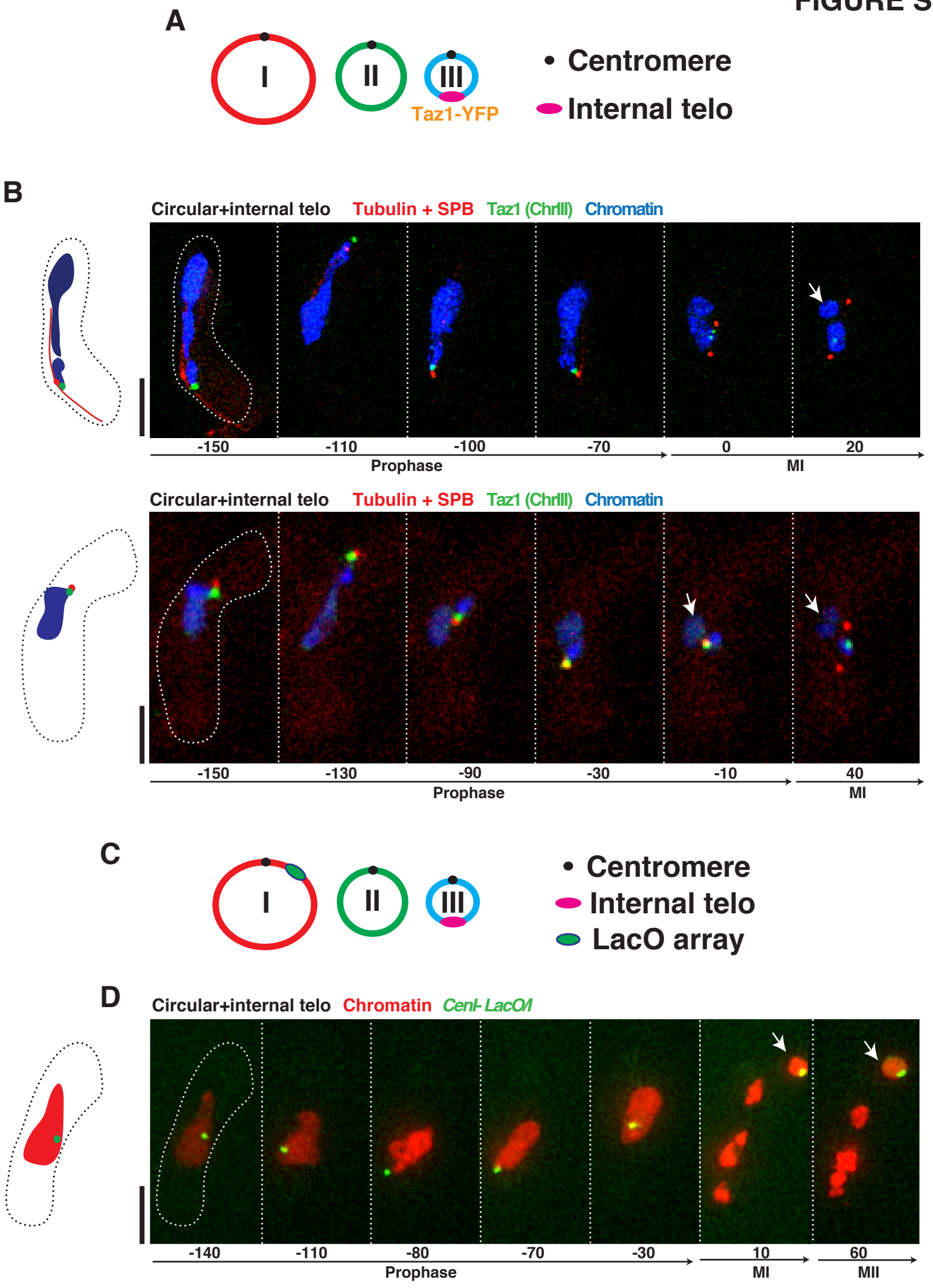
A
I
II
III
Taz1-YFP
Centromere
Internal telo
B
Circular+internal telo
Tubulin + SPB
Taz1 (ChrIII)
Chromatin
-150
-110
-100
-70
0
20
Prophase
MI
Circular+internal telo
Tubulin + SPB
Taz1 (ChrIII)
Chromatin
-150
-130
-90
-30
-10
40
Prophase
MI
C
I
II
III
Centromere
Internal telo
LacO array
D
Circular+internal telo
Chromatin
CenI-LacO/
-140
-110
-80
-70
-30
10
60
Prophase
MI
MII

FIGURE S9

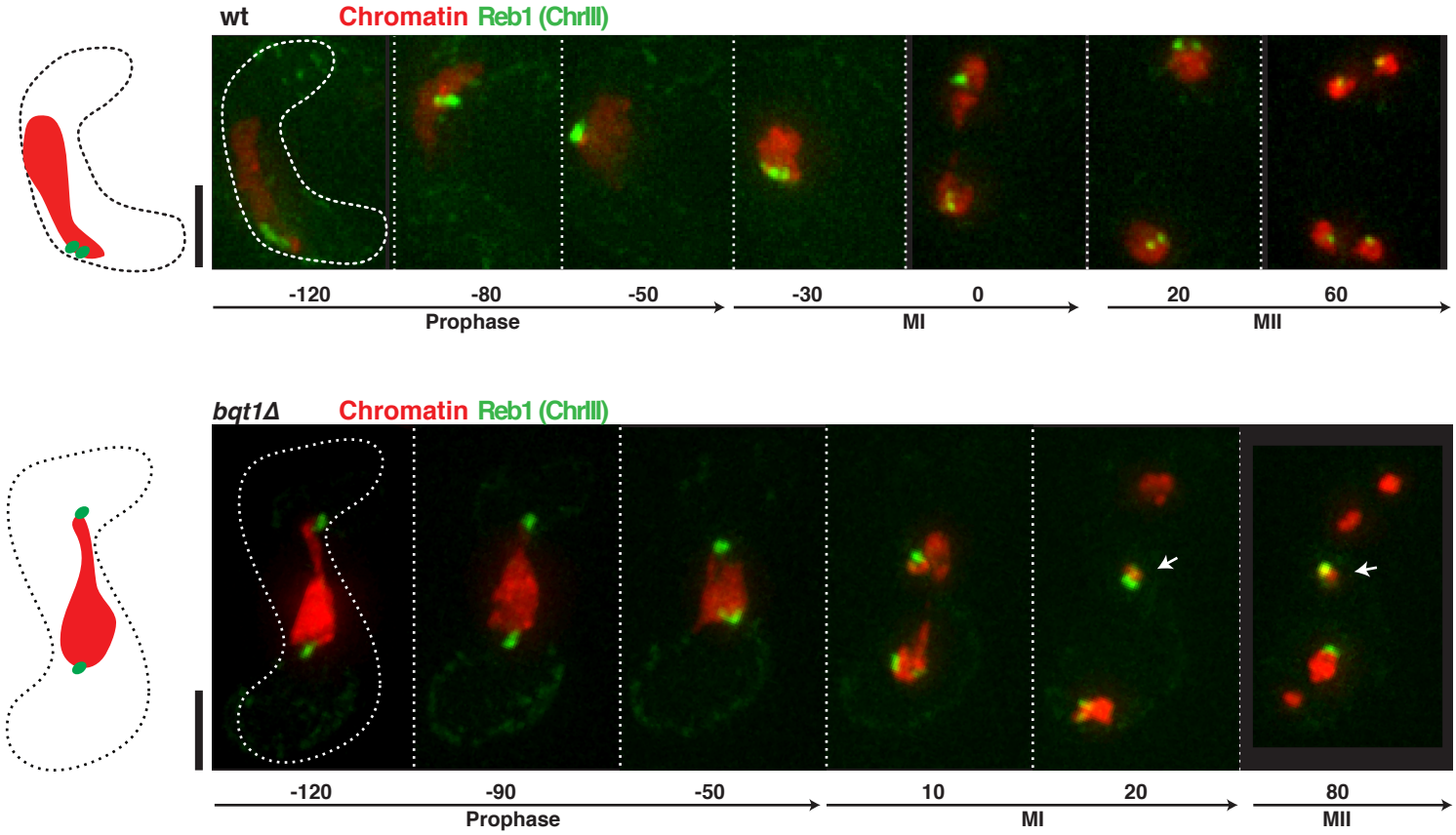
wt
Chromatin Reb1 (ChrIII)
-120
-80
-50
-30
0
20
60
Prophase
MI
MII
bqt1Δ
Chromatin Reb1 (ChrIII)
-120
-90
-50
10
20
80
Prophase
MI
MII

FIGURE S10

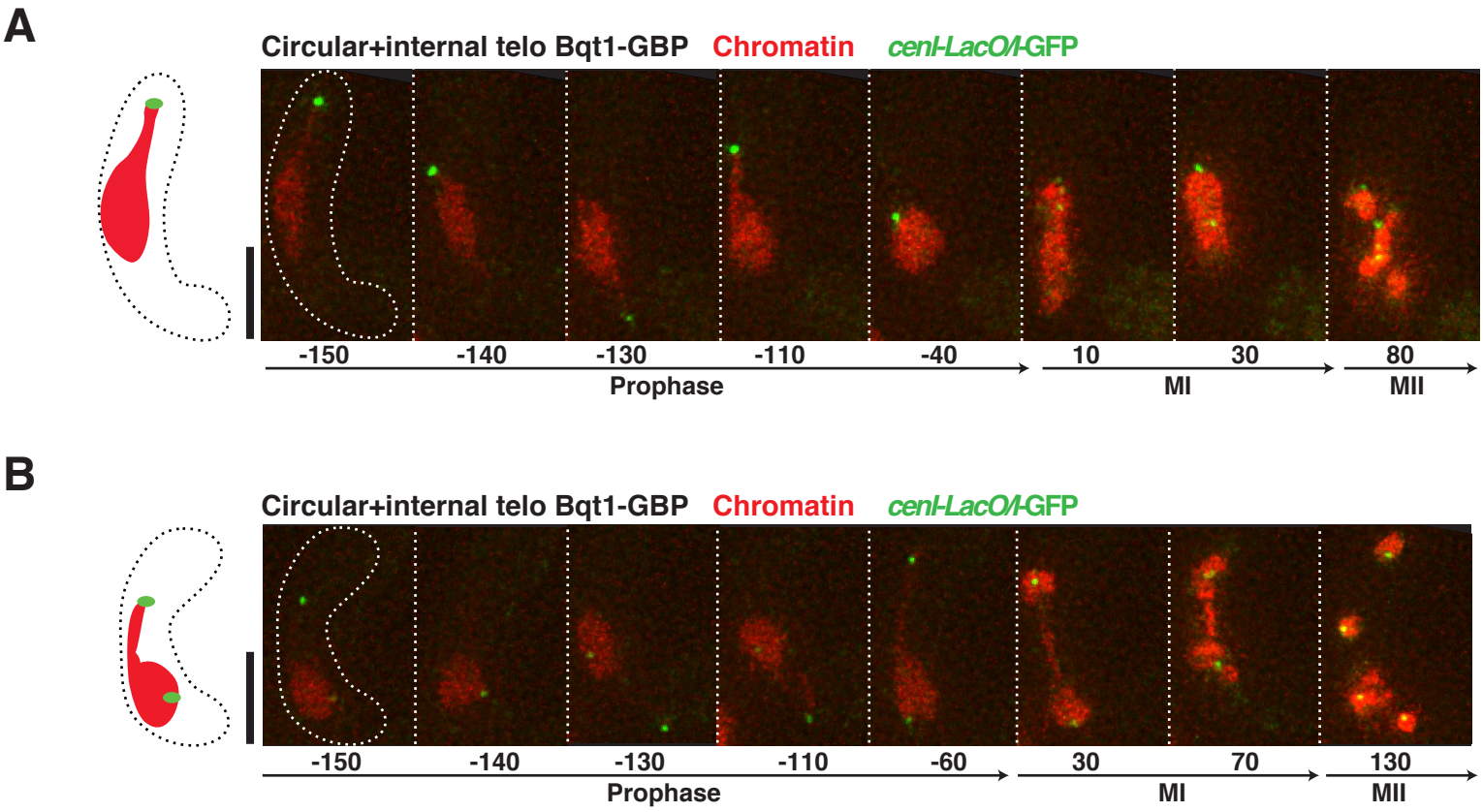
A
Circular+internal telo Bqt1-GBP
Chromatin
cenI-LacOI-GFP
-150
-140
-130
-110
-40
10
30
80
Prophase
MI
MII
B
Circular+internal telo Bqt1-GBP
Chromatin
cenI-LacOI-GFP
-150
-140
-130
-110
-60
30
70
130
Prophase
MI
MII

A

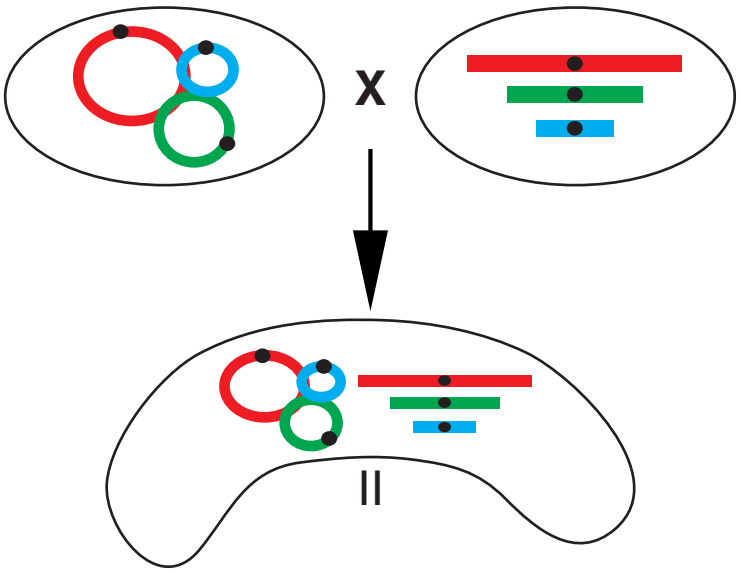
X
II

B

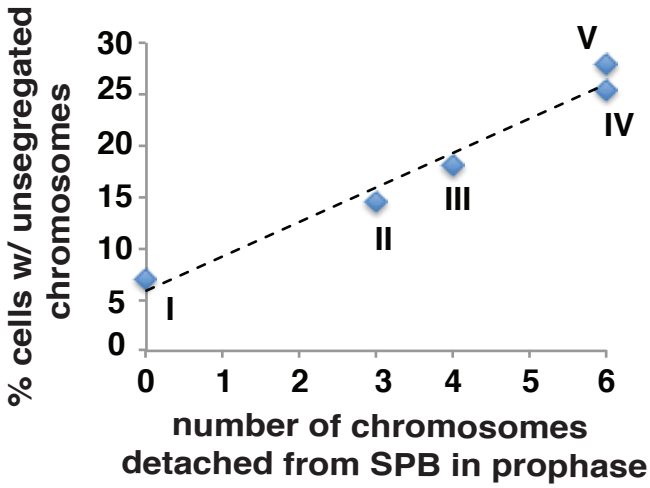
% cells w/ unsegregated chromosomes
30
25
20
15
10
5
0
0
1
2
3
4
5
6
number of chromosomes detached from SPB in prophase
I
II
III
IV
V

FIGURE S12

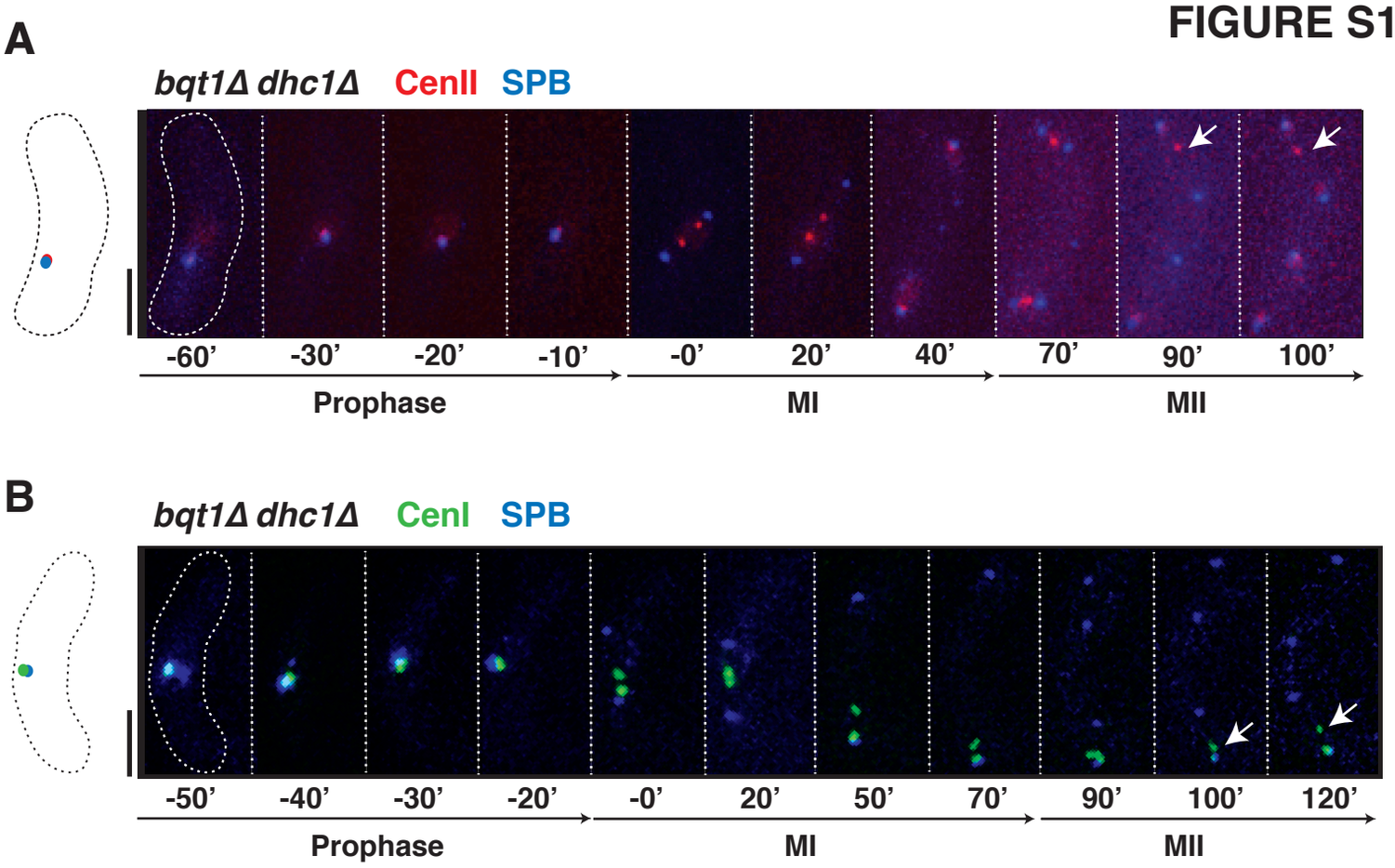
A
bqt1Δ dhc1Δ CenII SPB
-60’
-30’
-20’
-10’
-0’
20’
40’
70’
90’
100’
Prophase
MI
MII
B
bqt1Δ dhc1Δ CenI SPB
-50’
-40’
-30’
-20’
-0’
20’
50’
70’
90’
100’
120’
Prophase
MI
MII